Mechanisms of Development

Frizzled-3a and *slit2* genetically interact to modulate midline axon crossing in the telencephalon

Authors: Wolfgang Hofmeister[1], Christine A. Devine[1], Joseph A. Rothnagel[2] and Brian Key[1]

Authors addresses: [1]School of Biomedical Sciences and [2]School of Chemistry and Molecular Bioscience, University of Queensland, Brisbane, Queensland, 4072, Australia

Corresponding author: Prof. Brian Key
School of Biomedical Sciences,
University of Queensland
Brisbane 4072
Australia
TEL: +61-7-3365-2955
FAX: +61-7-3365-1766
brian.key@uq.edu.au

Figures and tables: 8 Figures, 4 tables, 4 supplementary Figures

Number of Pages: 27

Number of words: 5227

Key words: Frizzled-3, anterior commissure, post-optic commissure, slit2

Abstract

The anterior commissure forms the first axon connections between the two sides of the embryonic telencephalon. We investigated the role of the transmembrane receptor Frizzled-3a in the development of this commissure using zebrafish as an experimental model. Knock down of Frizzled-3a resulted in complete loss of the anterior commissure. This defect was accompanied by a loss of the glial bridge, expansion of the *slit2* expression domain and perturbation of the midline telencephalic-diencephalic boundary. Blocking Slit2 activity following knock down of Frizzled-3a effectively rescued the anterior commissure defect which suggested that Frizzled-3a was indirectly controlling the growth of axons across the rostral midline. We have shown here that Frizzled-3a is essential for normal development of the commissural plate and that loss-of-function causes Slit2-dependent defects in axon midline crossing in the embryonic vertebrate forebrain. These data supports a model whereby Wnt signaling through Frizzled-3a attenuates expression of Slit2 in the rostral midline of the forebrain. The absence of Slit2 facilitates the formation of a midline bridge of glial cells which is used as a substrate for commissural axons. In the absence of this platform of glia, commissural axons fail to cross the rostral midline of the forebrain.

1. Introduction

In bilaterally symmetrical animals, commissural axon connections ensure that neural activity on either side of the nervous system is integrated in order to generate appropriate behavioural responses. . While many mice mutant for axon guidance receptors and/or their signaling molecules exhibit defects in commissure formation (Lindwall et al., 2007), the mechanisms underlying the initial formation of these tracts are not well understood. Zebrafish provide a convenient model for deciphering the cell and molecular bases of commissural axon tract formation in vertebrates because of its rapid development and ease of imaging the stereotypical scaffold of axon tracts in the embryonic brain. The first commissural axons in the zebrafish brain form in a commissural plate within the rostral surface of the anterior neural tube. This plate contains the anterior and post-optic commissures which are established within 24 hours of fertilisation. The anterior commissure is pioneered by the telencephalic neurons of the dorsal rostral cluster which extend axons across the rostral midline (Chitnis and Kuwada, 1990; Wilson and Easter, 1991; Ross et al., 1992; Hjorth and Key, 2002). The diencephalic neurons of the ventral rostral cluster contribute axons to the post-optic commissure which grow across the rostral midline, ventral to the anterior commissure.

In mouse, Frizzled-3 (Fzd-3) is required for the formation of the anterior commissure as well as several other major forebrain tracts (Wang et al., 2002; Wang et al., 2006b). Frizzled-3 belongs to a family of seven-pass transmembrane receptors, known to bind members of the secreted Wnt ligand family via a highly conserved extracellular cysteine-rich domain (Bhanot et al., 1996; Dann et al., 2001; Widelitz, 2005). Frizzled receptors can activate at least three different signaling pathways depending on the Frizzled, Wnt ligand and co-receptor involved. These pathways result in the transcription of β-catenin target genes, changes in intracellular Ca^{2+} levels, or the polarization of cells orthogonal to the apical-basal axis. Fzd signaling acting through both the canonical and non-canonical signaling pathways is implicated in a diverse range of processes during development of the nervous system. Canonical Wnt signaling along with BMPs and FGFs play a role in neural induction and in the subsequent posteriorisation of the neural plate. Its antagonism by secreted frizzled related proteins (sFRPS) emanating from cells in the anterior neural border (ANB), the most rostral regions of the neural plate, is necessary in establishing the telencephalon (Houart et al., 2002). Later in neural development canonical signaling also plays a role in dorsal-ventral patterning of the telencephalon (Danesin et al., 2009). In contrast, non-canonical Wnt signaling has been linked to processes such as cell migration, neural tube closure

and axon guidance during neural development. Frizzled-3 provides an example of the multifaceted nature of Wnt/Frizzled signaling as it has been shown to be involved in all three pathways depending on the cellular context (Shedahl etal.,2003; Slursarki et al., 1997a; Slursarki et al., 1997b; Carron., 2003). In the nervous system it has been generally linked to planar cell polarity signaling such as neural tube closure (Wang et al., 2006a), axon guidance (Lyuksyutova et al ., 2003) and cell migration (Wada et al., 2006). More recently it has also been implicated as being required during sympathetic neuron development through its activation of β-catenin signaling (Armstrong et al., 2011). However, how zFzd3a acts in commissural plate development to ensure correct patterning of the neuroepithlium and thereby the appropriate expression of guidance molecules has not been studied as to date.

The chemorepulsive receptor Robo2 (Hutson and Chien, 2002) and its ligands Slit2 and Slit3 (Barresi et al., 2005) play a critical role in the formation of the post-optic commissure in zebrafish. These Slits appear to act as a chemorepulsive blanket that restricts axons to this defined commissural pathway. In addition, Slit2 and to a lesser extent Slit3 are required for the correct patterning of a population of Slit1a expressing glial cells in the zebrafish commissural plate. Loss of Slit2 or Slit2/Slit3 activity causes abnormal positioning of *slit1a*-expressing midline glia which leads to the aberrant growth of the commissural axons across the midline (Barresi et al., 2005). Slit2/3 presumably excludes Robo expressing glial cells from inappropriate regions (Barresi et al., 2005). In contrast, Slit1a appears to have a distinct function during commissure formation. Commissural axons are not repelled from *slit1a* expressing regions which suggests that Slit1a acts as a permissive cue or, at least, a less repulsive signal compared to Slit2/3 (Barresi et al., 2005). Thus the Slit family of guidance molecules have distinct yet crucial roles in commissure formation. Despite this, little is known as to how the expression of these guidance molecules is established in the commissural plate.

In the present study we found that zebrafish Frizzled-3a (zFzd3a) regulates the localisation of guidance cues in the rostral forebrain. Knock down of zFzd3a results in an expansion of *slit2* expression at the rostral midline, reduction or absence of the anterior commissure formation, an altered telencephalic-diencephalic midline boundary and a reduction or absence of midline glia. Simultaneous knock down of Slit2 and zFzd3a significantly rescued the anterior commissure defect, indicating *slit2* mis-expression is largely responsible for the absence of the anterior

commissure. Together, these results show that zFzd3a acts in the commissural plate to facilitate formation of the anterior commissure.

2. Results

2.1. Frizzled-3a is expressed in embryonic zebrafish brain

By 24 hours post-fertilisation, the embryonic brain of zebrafish is a blind ended tube containing a discrete set of neuronal clusters interconnected by axon tracts (Fig. 1A) (Hjorth and Key, 2002). There are two bilaterally symmetrical clusters of neurons in the forebrain at this age: the dorsorostral cluster in the telencephalon and the ventrorostral cluster in the ventral diencephalon. Each pair of neuronal clusters is interconnected on either side of the forebrain via the anterior commissure and the post-optic commissure, respectively. The zebrafish homologue of *frizzled-3a* (*zfzd3a)* was cloned and a 750 bp riboprobe was generated to analyse expression in embryonic brains by wholemount *in situ* hybridization. *zfzd3a* was expressed in the neuroepithelium of both the presumptive telencephalon and ventral diencephalon (Fig. 1B). In the telencephalon the expression of *zfzd3a* extended from the anterior commissure through the dorsorostral cluster to the dorsocaudal margins of this brain region. In the ventral diencephalon *zfzd3a* was expressed from the post-optic commissure, through the ventrorostral cluster and into the trajectory of the tract of the post-optic commissure (Fig. 1B). *zfzd3a* was also widely expressed in the mesencephalon and rhombencephalon (Fig. 1B) as previously observed in the mouse brain (Wang et al., 2002; Wang et al., 2006a).

Next we examined the spatial relationship between *zfzd3a* expression in the commissural plate (rostral surface of the brain) and the trajectories of the anterior and post-optic commissures by confocal laser scanning microscopy (Fig. 1C-H). Flat mounts of the rostral brain enabled the anterior and post-optic commissures to be scanned in the same plane. Using this approach *zfzd3a* was found to be diffusely expressed by the neuroepithelium of the commissural plate. The strongest expression was detected in the regions dorsal to the anterior and post-optic commissure (Fig. 1E). Control embryos incubated with sense RNA probes revealed negligible background staining (Fig. 1F-H).

2.2. Loss of zFzd3a perturbs formation of the forebrain commissures

We used an antisense morpholino knock down approach to examine the role of zFzd3a in early commissural formation in the embryonic forebrain. Two independent morpholinos (MOs)

referred to as *zfzd3a*-UTR and *zfzd3a*-AUG were generated against the 5' untranslated region of *zfzd3a* mRNA (Fig. 2A; Table I). A randomly scrambled MO was used for control injections (Table I). We tested the efficacy of the *zfzd3a* MOs by examining their ability to knock down the expression of GFP from a plasmid construct (Fig. 2A). The GFP coding region was cloned downstream of the target untranslated region recognized by the two MOs. When 50pg of this construct (*zfzd3a*-UTR-GFP) was injected alone or together with standard control MO into zygotes, GFP was mosaically expressed throughout the embryo at 24 hours post-fertilisation (n=45/59; Fig. 2B, E). In contrast, co-injection of the construct with either 3.5ng of *zfzd3a*-UTR MO (n=38; Fig. 2C, F) or 1.25ng of *zfzd3a*-AUG MO (n=41; Fig. 2D, G) resulted in the complete loss of GFP expression. This loss of GFP fluorescence confirmed that both *zfzd3a* MOs bound to their designed target sequence and were able to block translation of mRNA.

Animals injected with up to 5 ng of control MO displayed normal wild-type formation of the anterior commissure (Fig. 2H). In contrast, injection with either the 3.5 ng *zfzd3a*-UTR or 1.25 ng *zfzd3a*-AUG MO resulted in a significant increase in embryos with a loss of the anterior commissure (44-55% penetrance). Some embryos also showed reduced crossing of the POC (unfilled arrows, Fig 2 I-L) in addition to a loss of the AC, however the reason for this defect remains unclear. It should be noted that we only examined animals that were not developmentally delayed and exhibited normal gross body morphology. While axons appeared to project partially into the anterior commissure they typically failed to cross the rostral midline of the brain (arrowheads, Fig. 2I, J). Most axons appeared to stall prior to reaching the midline. . Taken together, the use of two independent antisense morpholinos that produced similar phenotypes, the fact that these morpholinos knocked down GFP expression from constructs containing *zfzd3a* target sequences, and that the anterior commissure defect observed in mice was recapitulated in zebrafish indicate the specificity of the morpholinos. Interestingly, a single line of zebrafish carrying a point mutation in *zfzd3a* has been previously generated by *N*-ethyl-*N*-nitrosourea mutagenesis (Wada et al., 2006). Although the hindbrain phenotype in this line of zebrafish could not be rescued by injection of full-length mRNA line, it was recapitulated by a dominant negative truncated construct. We observed the same morpholino-induced anterior commissure phenotype when embryos were injected with 375pg of mRNA encoding a dominant negative form of mouse Frizzled-3, but not in control embryos injected with an equivalent amount of GFP (data not shown). The dominant negative mouse Frizzled-3 was synthesized from a splice variant of mouse Frizzled-3 containing a premature stop signal following the cysteine rich domain. These results further confirmed the specificity of our morpholino knock

down approach. We have adopted the anti-sense morpholino approach here as it has allowed us to examine various gene-gene interactions underlying the phenotype (see below).

Previous reports have shown the possibility of off-target effects resulting from morpholinos due to activation of the p53 apoptotic pathway (Robu et al., 2007; Gerety et al., 2011). To ensure this was not the case we co-injected 2.0ng zFzd3a-AUG MO with p53 MO (5ng) to block p53 activation (Fig. 2K-L). Co-injection with p53 MO did not reduce the penetrance (Table II) or severity (Fig. 2L) of the AC defect (unfilled arrowhead, Fig. 2L. . Thus, the loss of the AC observed following knock down of zFzd3a is not due to off-target activation of p53. To further test whether our AC defect was specific to knock down of Frizzled-3 we co-injected 2.0ng of zFzd3a-ATG MO with 375pg of mouse *fzd3* mRNA which lacked the morpholino binding sequence. Injection of 2.0ng of zFzd3a-ATG MO alone resulted in an absent or severely reduced AC in 76% of embryos (unfilled arrowhead, Fig. 2K) Co-injection of the morpholino with *mfzd3* mRNA significantly reduced the percent of embryos with a loss of the AC. Rescued embryos showed the formation of a distinct fascicle in the AC (unfilled arrow head, Fig. 2M).. These results confirmed that loss of the AC was specifically due to knock down of *zFzd3a.*

2.3. Loss of zFzd3a affects glial bridge formation

A local glial cell population has been shown to act as a substrate for axon growth (Barresi et al., 2005). To assess the patterning of these midline glia we used a previously characterized rabbit anti-GFAP antibody (Nona et al., 1989). In control embryos, *slit1a* expressing GFAP positive (+) glia underlie the AC (Barresi et al., 2005) (Fig. 3A-C, supplementary Fig S1). Following knock down of zFzd3a, GFAP+ glia (unfilled arrowhead, Fig. 3E; Fig. 3F) as well as AC axons (unfilled arrowhead, Fig. 3D; Fig. 3F) are lost from the midline. Embryos injected with zFz3a-AUG MO and mFzd3a mRNA showed a significant rescue of both the commissural axon and glial bridge defects (Fig. 3G-I).

2.4. Loss of zFzd3a causes expansion of the *slit2* expression domain in the telencephalon

Slit2 has previously been shown to play a role in commissure formation by acting as a repulsive cue for commissural axons and a subset of GFAP+ midline glia (Barresi et al., 2005). Thus, we next investigated whether the loss of commissural axons and glial cells at the midline of the AC was accompanied by abnormal expression of *slit2* in this region. In wildtype embryos *slit2* is

principally expressed in a restricted triangular-shaped domain of neuroepithelium (dashed outline, Fig. 4A) in the region surrounding the anterior commissure (Fig. 4B-C). By analyzing single optical slices obtained by confocal laser scanning microscopy we revealed that the axons in the anterior commissure crossed the midline within neuroepithelium that was not expressing *slit2* (Fig. 4D-F). The *slit2* positive cells lay deeper beneath the axons of the anterior commissure. Following knock down of zFzd3a, *slit2* became more strongly and widely expressed in the neuroepithelium (dashed outline, Fig. 4G, M). Embryos with expanded *slit2* expression had either a complete loss of axons (arrowhead, Fig. 4H, I) or exhibited few crossing axons (arrowhead, Fig. 4N, O) in the anterior commissure. Analysis of single optical slices revealed ectopic expression of *slit2* in the typically *slit2*-negative neuroepithelium where anterior commissure axons would normally cross the midline (compare Fig. 4D and 4J, and 4F and 4L). Uncrossed axons could be observed at the edge of this ectopic *slit2* domain (arrowheads, Fig. 4K). The merged images revealed that the anterior commissural axons did not enter into the expanded domain of *slit2* expression (Fig. 4L). Similar results were obtained with both MOs (Fig. 4G-I and M-O; Table III).

2.5. Loss of zFzd3a affects formation of the commissural plate

Previous studies have shown that *shh* is involved in patterning of *slit* expression and glial formation in the rostral forebrain (Barresi *et al.,* 2005). We show here that *shh* is expressed in the wedge-shaped domain of neuroepithelium in the diencephalon beneath the POC (Fig. 5A-C) and weakly in two small patches lateral to the midline of the telencephalon (dashed yellow outline, Fig. 5A). One possibility is that aberrant expression of *shh* may account for some axon guidance defects as previously described (Barresi et al., 2005). However, we found no difference in *shh* expression between control embryos or embryos injected with zFzd3a-AUG MO (compare Fig. 5A to G). Thus *shh* does not appear to be involved in *zfzd3a*-dependent axon guidance across the rostral midline. Next we asked if *zfzd3a* was not only affecting the distribution of glial cells and the expression of *slit* guidance molecules but whether it was also affecting the morphology of the midline. We scanned the optic recess of control animals at higher resolution (Fig. 5D-F and supplementary Fig S2) which revealed the presence of a distinct linear border between cells of the telencephalon and diencephalon. Following knock down of zFzd3a we found that the optic recess was severely disrupted at the midline (Fig. 5J-L and supplementary Fig. S2.). The junctional border between the telencephalon and diencephalon appeared to be expanded (demarcated by arrowheads in Fig. 5K) by the presence of a

disorganized array of cells. Since *netrin1* is expressed within this region (Lauderdale et al., 1997; Strähle et al., 1997) we next examined its distribution in control and zFzd3a knock down embryos. We showed that *netrin1a* was expressed by cells lying dorsal to the optic recess and ventral to the anterior commissure in the rostral forebrain (Fig. 6 A-C). A similar expression pattern was observed for *netrin1b* (supplementary Fig. S3A-C). Following knock down of zFzd3a, *netrin1a* expression expanded dorsolaterally (filled arrows, compare Fig. 6D with 6A) into the region which also now expressed *slit2* (compare with Fig. 4G-O). In addition, the ventral borders of *netrin1a* (Fig. 6D-F) and *netrin1b* (supplementary Fig. S2D-F) expressing domains were no longer linear but displayed a distinctive lip about the midline, which was consistent with the abnormal morphology we previously noted in this region (Fig. 5K). The ectopic cells that filled this split optic recess do not express either *netrin1a* (Fig. 6D) or *netrin1b* (supplementary Fig. 3D). Taken together, our data suggests that there is aberrant formation of the commissural plate following knock down of *zFzd3a*. There is expansion of *slit2* expression and the abnormal presence of *netrin1* negative ectopic cells within the optic recess. This abnormal expression is specific to the commissural plate as analysis of markers involved in specification of regional brain territories appeared grossly normal following knock down of zFzd3a (supplementary Fig. S4)

2.6. Knock down of Slit2 rescues the anterior commissure phenotype produced by loss of zFzda

Since Slit2 acts as a repulsive cue for axons and glia and because the absence of the anterior commissure is correlated with mis-expression of *slit2* we proposed that Slit2 was causative in the *zFzd3a* phenotype. To investigate whether increased expression of *slit2* in the commissural plate was indeed responsible for disruption of the anterior commissure following knock down of zFzd3a we decided to rescue the phenotype by simultaneous knock down of Slit2. If expansion of *slit2* expression was responsible for the anterior commissure phenotype then knock down of Slit2 should allow these axons to cross the midline. Embryos were injected with either 6.25ng standard control MO alone (Fig. 7A), 5ng *slit2*-AUG MO alone (Fig. 7B-C), 1.25ng *zfzd3a*-AUG MO alone (Fig. 7D-E), or 1.25ng *zfzd3a*-AUG MO and 5ng *slit2*-AUG MO together (Fig. 7F-G).

Knock down of Slit2 resulted in axons defasciculating and aberrantly projecting into the neuroepithelium between the two commissures (arrowhead, Fig. 7B-C), which is consistent with previous reports (Barresi et al., 2005). Although in some embryos this defasciculation reduced the size of the anterior commissure (Fig. 7B), it was never completely ablated (arrow, Fig. 7B). We therefore categorised anterior commissure defects into four different classes: (I) complete loss or failed formation; (II) marked reduction in fascicles or reduced formation; (III) crossing of the anterior commissural axons together with aberrant projection of some axons into the surrounding neuroepithelium; and (IV) normal formation. Knock down of Slit2 did not result in a significant loss or reduction of the AC, as penetrance of Class I or Class II embryos was not altered compared to control embryos (Table IV). However, knock down of zFzd3a significantly increased the incidence of embryos with a failed or severely reduced anterior commissure, as shown by an increased penetrance in Class I (arrow in Fig. 7D; 60%, n=24; Table IV) or Class II (arrow in Fig. 7E; 5%, n=10; Table IV) phenotypes in comparison to controls (Fig. 7A). Simultaneous knock down of both Slit2 and zFzd3a significantly decreased the proportion of embryos with a loss of the anterior commissure (Class I phenotype;Fig. 7F and G; 16%, n=6, p<0.001; Table IV). Rescue of this phenotype indicated that the increased expression of *slit2,* associated with the knock down of zFzd3a, was indeed responsible for the aberrant formation of the anterior commissure. The misprojecting axons observed in the neuroepithelium surrounding the commissures in the double knock downs (arrowheads, Fig. 7F and G) was due to the reduction of *slit2* since these aberrant axons were observed in the single Slit2 knock down embryos (arrowheads in Fig. 7 B-C).

3. Discussion

The mammalian anterior commissure is highly vulnerable to genetic perturbations in a number of axon guidance receptors and ligands as well as their associated signaling pathway molecules including Netrin-1 (Serafini et al., 1996), DCC (Fazeli et al., 1997), EphA4 (Kullander et al., 2001), Sema3B and 3F (Falk et al., 2005), Nrp2 (Falk et al., 2005), NrCAM (Falk et al., 2005), Plexin-A4 (Suto et al., 2005), Fzd3 (Wang et al., 2006), Trio (Briancon-Marjollet et al., 2008), Rac1 (Kassai et al., 2008) and Celsr3 (Zhou et al., 2008). The lack of redundancy between these different axon guidance molecules suggests that each acts discretely during formation of this commissure. Unfortunately our understanding of the role of these different genes in the guidance of axons across the rostral midline is fragmentary. In the present study we analysed the

cell and molecular mechanisms underlying the role of Fzd3 in the development of the anterior commissure using zebrafish as an experimental model. We show that zFzd3a influences the localisation of midline glia and the expression of guidance molecules in the commissural plate during the guidance of axons across the rostral midline. We also show that expansion of the *slit2* expression domain following knock down of zFzd3a is responsible for the absence of the anterior commissure. How zFzd3a acts to confine *slit2* expressing cells at the appropriate regions of the midline is uncertain. The expansion of *slit2* and loss of the local glia population could be a consequence of aberrant morphogenetic movements at the rostral midline or due to inappropriate specification of midline cells.

3.1. zFzd3a patterns the commissural plate and controls midline axon *crossing*

The rostral surface of the embryonic vertebrate brain or commissural plate contains the anterior and posterior commissures which lie dorsal and ventral to the telencephalic-diencephalic boundary demarcated by the optic recess. Axons in both of these commissures grow across a substrate or bridge of glial cells and *shh* induced perturbations in the migration of these glia are known to affect commissural formation (Barresi et al., 2005). The zebrafish homologue of Fzd3, is expressed by the neuroepithelial cells of the commissural plate. Consequently, knock down of zFzda3a led to loss of the anterior commissure which phenocopied the effects of Fzd3 loss-of-function previously reported in the mouse brain (Wang et al., 2002). We further revealed that telencephalic neurons in zebrafish projected axons rostrally within the initial pathway of the anterior commissure in the absence of zFzd3a. Thus, zFzd3a does not appear to be important for axon outgrowth per se, but is rather required for midline crossing during commissure formation. This is consistent with reports that dissociated neurons cultured from embryonic Fzd3 knock-out mice grow normally and display normal axonal and dendritic morphology (Wang et al., 2002).
.

Our results show that in contrast to the chemoattractant role of Fzd3 in spinal cord commissural axons of mice (Lyuksyutova et al., 2003), the zebrafish orthologue Fzd3a acts to regulate

patterning of the commissural plate thereby indirectly influencing axon guidance. We have shown here that knock down of zFzd3a resulted in a loss of glia within the pathway of the anterior commissure, suggesting that the loss of the anterior commissure is due to abnormal localization GFAP+ glia in the commissural plate. These glial defects arose from an aberrant and expanded expression of *slit2* in the rostral midline which then led to axon guidance defects in this commissure. This patterning defect was highly localized to the rostral midline, as the gross regionalisation of the forebrain, as indicated by the expression patterns of *hlx*, *wnt1*, *shh*, *pax6*, *dlx2* and *emx*, was unaltered. The significance of the expanded expression of *slit2* was revealed when the midline crossing defects were rescued by the simultaneous knock down of zFzd3a and Slit2. Thus zFzd3a acts to regulate *slit2* distribution within the neuroepithelium which when perturbed affects the formation of glial bridges thereby indirectly regulating axon navigation in the anterior commissures (Fig. 8).

The GFAP positive glial cells that reside in the zebrafish midline express *slit1a* (Barressi et al ., 2005) and presumably act as an axon growth substrate as in the zebrafish tectum (Xiao et al., 2011). Consequently, along with a loss of midline glia in zFzd3a knock down embryos we also observed a reduction in *slit1a* expression (Supplementary Fig. S1). These glia also express a combination of Robo receptors which are known to bind the Slit family of proteins (Barressi et al., 2005). Most likely it is the expression of these receptors that causes their exclusion from regions of *slit2* expressing neuroepithelium (Barressi et al., 2005). Thus Slit2 presumably acts as a repulsive guidance cue for glia as well as for axons. This results in the inability of glial cells to migrate to the midline due to the expansion of repulsive *slit2* in zFzd3a knock down embryos. Specification of glia does not appear to be an issue as GFAP staining confirms their presence in more lateral regions of the commissural plate (Fig. 4).

The expansion of *slit2* that we observed in the commissural plate was not due to aberrant expression of *shh*, which is expressed normally despite the absence of the anterior commissure in zFzd3a knock down embryos. In addition to aberrant expression of *slit2* we also observed spatial changes in expression of *netrin1a* and *netrin1b* and the appearance of ectopic midline cells in the commissural plate. These ectopic cells expand the optic recess and appear similar to the aberrant midline cells observed in the neural keel following knock down of planar cell polarity pathway components (Ciruna *et al.*, 2006). It is possible that these ectopic cells contribute to the disruption of the *slit2* and *netrin* expression domain by disrupting the appropriate morphogenetic movements required to form the commissural plate.

In wild-type embryos the triangular shaped *slit2* expression domain surrounds the AC and forms a channel so that the axons cross in a region devoid of *slit2* neuroepithelial cells. In contrast, knock down of zFzd3a results in *slit2* positive neuroepithelial cells being present where axons normally cross. Whether the localization of the *slit2* message reflects the expression of Slit2 protein could not be ascertained as no working antibody was available. Since Slit2 is a secreted protein it is possible that in wild-type embryos the protein itself is in closer proximity to the commissural axons than suggested by the *in situ* hybridisation experiments. Nevertheless, the expansion of *slit2* positive neuroepithelium in zFzd3a knock down embryos suggests that the protein is now secreted in an expanded region compared to control embryos.

In embryos injected with only the *slit2* morpholino, commissural axons aberrantly coursed into the region between the anterior and post-optic commissures as previously described (Barresi et al., 2005). These results support the previously proposed "surround repulsion" model of Slit2 function in the zebrafish optic commissure whereby Slit2 surrounds the commissure and forces axons to grow on a substrate of neuroepithelium not expressing this chemorepellent (Hutson and Chien, 2002) (Fig. 8A). This model is also supported by the inability of anterior commissural axons to cross the midline following the loss of zFzd3a and the resulting ectopic expression of *slit2* in the neuroepithelium which normally supports the growth of these axons (Fig. 8B). In this case, the expansion of the *slit2* zone in zFzd3a loss-of-function embryos caused axons to stall or turn prior to entering the anterior commissure. These zFzd3a mediated changes in *slit2* expression are similar to the hedgehog mediated changes in *slit2* expression observed previously in the pathway of the post-optic commissure (Barresi et al., 2005). Loss of hedgehog signaling in *gli* mutants caused expansion of *slit2* expression, mis-patterning of midline *slit1a*-expressing glia and defasciculation of the post-optic commissure (Barresi et al., 2005). However, we have shown here that *zFzd3a* causes preferential effects on expression of *slit2* in the anterior commissure which are unrelated to *shh*.

4. Experimental procedures

4.1. Zebrafish maintenance

Zebrafish were maintained on a 14 hour light and 10 hour dark cycle at the University of Queensland fish facility. Light induced mating of adult fish was used to obtain embryos.

4.2. Isolation of full length zFzd3a and in situ hybridization probes

zfzd3a was isolated from zebrafish random primed cDNA using primers designed to the putative *frizzled* fragment. 5' and 3' regions were subsequently isolated using a Rapid Amplification of cDNA ends protocol followed by polymerase chain reaction (Frohman et al., 1988) and then sequenced. Overlapping fragments were joined to create the full-length mRNA sequence (Genbank accession number DQ200953). This sequence was used to design a 750bp *in situ* probe covering 500bp of the C-terminal end and 300bp of the 3' UTR of *zfzd3a* mRNA. BLAST analysis revealed that this region had the greatest variance between *frizzled* homologues. Gene specific primers 5'-AGT GGG CCA GTT TCT TCA GTG-3' and 5'-GTT TGG TAT CCT CTG ATT TGG-3' were used to amplify the probe cDNA (corresponding to fragment 1998bp-2747bp of DQ200953). For cloning of a Slit2 contruct, to be used as a template for riboprobe synthesis, a 2.4kb fragment was amplified from cDNA using primers 5'-ACA TTG AAC TTG CTG GGC CCA-3' and 5'-CGA CAC GCC ATC TCT CTG T-3'. PCR products were subsequently gel extracted and cloned into pGemT-easy (Promega Corporation, Madison, WI, USA) for generation of riboprobes.

4.3. Morpholino and DNA microinjections

Morpholino (MO) phosphodiestermer oligonucleotides were purchased from Gene Tools LLC (Philomath, OR). Two non-overlapping translational blocking morpholinos were designed against *zfzd3a* (Table I). Morpholinos were used to allow precise control of protein knockdown through titration of the MO amount, as opposed to the use of truncation mutants where the biological consequence of cellular protein aggregates failing to reach the membrane is difficult to ascertain (Wada et al., 2006). A control morpholino which does not bind to zebrafish transcripts was used as a test for non-specific effects (Table I). To suppress any potential off-target effects induced by some MOs due to p53 activation, a previously published MO to block p53 (Table I)

15

was used (Robu et al., 2007). For knock down of Slit2a, a morpholino designed against the 5' UTR region was used (Table 1) that phenocopied the commissural axon guidance defect of a previously published morpholino (Barresi et al., 2005), without affecting other developmental processes MOs were resuspended in sterile water at a concentration of either 50mg/ml or 25mg/ml and then stored at -20°C. The stock solution was diluted to the desired concentration in water and injected into the yolk of 1-4 cell staged embryos. For combinatorial knock down experiments, zFzd3a MO, Slit2 MO and Std-cont MO were loaded into separate needles and embryos were injected with either zFzd3a MO and control MO, or Slit 2 MO and control MO, or zFzd3a MO and slit2 MO. This approach ensured the total amount of morpholino injected remained constant. Std-cont MO alone was also injected into control embryos at matched concentrations. For the MO rescue experiment, zFzd3a-AUG MO and mFzd3a mRNA were loaded in different needles for injection which ensured that the same amount of MO was delivered to embryos injected with MO alone or with MO and mRNA.

An enhanced green fluorescent protein (eGFP) reporter construct was used to test the efficacy of *zfzd3a*-UTR MO and *zfzd3a*-AUG MO. The 5'UTR and coding sequence containing the MO target sequences was cloned upstream of eGFP in the pCS2+ vector (Turner and Weintraub, 1994). Plasmids were co-injected with standard control or *zFd3a* MOs into the cytoplasm of 1-cell embryos at a final concentration of 70 ng/μl.

4.4. mRNA microinjection

Capped poly-adenylated mRNA was synthesized using the SP6 message mMachine kit (Ambion Inc., TX). *zfzd3a and mfzd3* cDNA was cloned into the pCS2+ plasmid and linearised at the 3'end of the inserted sequence via enzymatic digestion with *Not-1* before being transcribed *in vitro*. The transcribed mRNA was diluted to an appropriate concentration in nuclease free water before injection into the yolk of the embryo at the 1-cell stage at a volume of 0.5-1nl.

4.5. In situ hybridization and immunofluorescence

Dioxigenin-labeled anti-sense RNA probes were synthesized from T7/SP6 transcription initiation sites using a commercially available kit (F. Hoffman-La Roche Ltd., Basel, Switzerland). The

following probes were generated: *zfzd3a*, *pax6* (Krauss et al., 1991), *wnt1* (Molven et al., 1991), *emx1* (Kawahara and Dawid, 2002), *dlx2* (Akimenko et al., 1994), *hlx1* (Fjose et al., 1994) *shh* (Krauss et al., 1993)*, slit1a* (Hutson *et al.,* 2003), *slit2*, *netrin1a* (Lauerdale *et al.,* 1997) and *netrin1b* (Strähle et al., 1997). Gene expression patterns were visualised using Nitro-blue tetrazolium chloride and 5-Bromo-4-chloro-3-indolyl phosphate (F. Hoffman-La Roche Ltd., Basel, Switzerland). Staining with the *slit2* riboprobe was identical to previously published expression patterns (Miyasaka et al., 2005)

Immunocytochemical labeling of wholemount zebrafish brains with acetylated α-tubulin was performed as previously described (Devine and Key, 2003) using an anti-mouse IgG conjugated to Alexa 594 secondary antibody (1:200). To label glial cells a rabbit anti-goldfish GFAP antibody was used (Nona et al., 1989) as previously described (Barresi et al., 2005). Wholemount *in situ* hybridization using Fast Red (F. Hoffman-La Roche Ltd.) as a substrate combined with HNK-1 or acetylated α-tubulin immunocytochemical staining was described previously (Hjorth and Key, 2001; Barressi et al., 2005). Fluorescence labeled brains were mounted laterally or anteriorly between two coverslips and serial parasagittal optical sections were collected every 1μm using a Zeiss LSM 510 laser scanning confocal microscope or a Biorad MRC-1000 confocal microscope. The z-stacks were compiled using Zeiss-LSM software or Image-J (Abramoff et al., 2004). The significance of difference in penetrance of phenotypes was assessed using Fisher's exact test. Analysis of mean fluorescence values of *slit1a* expression levels was performed on control and experimental embryos processed for *in situ* hybridization under identical conditions. Confocal images were subsequently collected using the same microscope settings and mean fluorescence values were obtained using Image-J software. The significance of differences in levels was examined using Student's t-test.

Fig. 1. *zfzd3a* **expression in the brain at 24-28 hours post-fertilization (hpf)**. (A) Lateral view of the 24hpf brain demonstrating the major axon tracts. Neurons in the dorsorostral cluster (drc) project axons across the midline via the anterior commissure and ventrally via the supraoptic tract (SOT). The ventrorostral cluster of neurons projects rostrally across the midline via the post-optic commissure and caudally via the tract of the post-optic commissure (TPOC). The epiphyseal cluster (ec) projects ventrally via the dorsoventral diencephalic tract (DVDT). The ventrocaudal cluster (vcc) projects axons into the medial longitudinal fascicle (MLF) and the ventral commissure (VC). Axons of the tract of the posterior commissure (TPC) cross the dorsal midline via the posterior commissure (PC). (B) *In situ* hybridisation using a probe specific to *zfzd3a* shows expression of the transcript throughout the mid (mesencephalon; me) and hindbrain (rhombencephalon; rh) (n=7). In the forebrain, expression is strongest in the telencephalon (te) and in ventral diencephalon (di) (dashed outline). The commissural plate was simultaneously examined for expression of (C) HNK-1 to label axons and (D) *zfzd3a*. HNK-1 depicts the anterior comissure (AC) and the post-optic commissure (POC) as well as the intervening optic recess (OR). A merged image is presented in panel (E) with axons in green and zfzd3a in red (n=5). Strongest *zfzd3a* expression was detected both dorsal to the anterior commissure (stars) and the post-optic commissure (stars). (F-H) Hybridisation using sense control RNA did not result in any background non-specific staining. Rostral is facing and dorsal to the top in all panels. Scale bar in E is 20μm.

Fig. 2. Knock down of zFzd3a results in loss of the anterior commissure Embryos were injected with 5ng of Std-cont MO, 3.5ng of zFzd3a-UTR MO or 1.25ng of zFzd3a-AUG MO at the 1-4 cell stage and raised to 28hpf-30hpf. To ensure morpholinos block zFzd3a translation a GFP reporter construct containing the MO target sites upstream of the GFP coding sequence was constructed (A). Embryos injected with 50pg of zFzd3a (UTR)-GFP plasmid and Std-cont MO showed mosaic GFP fluorescence at 28hpf (B, E). Embryos injected with either 3.5ng of Fzd3a-UTR MO (C, F) or 1.25ng of zFzd3a-AUG MO (D, G) and 50pg of zFzd3a (UTR)-GFP did not show GFP fluorescence, indicating the ability of either morpholino to block protein translation. The commissural plate was labeled with anti-acetylated tubulin to visualise the anterior commissure (AC) and the post-optic commissures (POC) (H-M). Rostral is facing and dorsal is to the top in these panels. Control embryos show the distinct formation of commissures (H). In contrast, following injection of either of the two zFzd3a MOs defects were observed in the formation of the anterior and post-optic commissures (I-K). Knock down of zFzd3a resulted in a loss of the anterior commissure (unfilled arrowhead, I-K) and in some cases a reduction and

disorganization of the POC crossing axons (unfilled arrow, I, J). Co-injection of zFzd3a-AUG MO with p53 MO did not change the severity of the AC defect (unfilled arrowhead L). In contrast Co-injection of zFzd3a-AUG MO with *mfzd3a* RNA resulted in significant reduction in the number of embryos with a loss or severe reduction of the AC (Table II). Rescued embryos showed a clear formation of an AC fascicle (unfilled arrowhead, M). Scale bar in M is 20μm.

Fig. 3. Abnormal commissure formation correlates with abnormal patterning of glial bridges. Compiled confocal sections of wholemount zebrafish brains at 28-30hpf stained for GFAP (B,E,H and in red C,F,I) and acetylated tubulin (A,D,G and in green C,F,I). Rostral is facing and dorsal to the top in all panels. Embryos were injected with Std-cont MO (A-C), zFzd3a- AUG MO (D-F) or zFzd3a-AUG MO and *mfzd3* mRNA. In control embryos GFAP spans the midline where the AC and POC cross acting as a growth substrate. Knock down of zFzd3a results in an absence of glial cells where the AC normally forms coinciding with an absence of the tract (unfilled arrowheads in D and E). Embryos where the AC has been restored with ubiquitous expression of mFzd3a show the reestablishment of the glial bridges associated with the AC. Scale bar in C is 20μm.

Fig. 4. zFzd3a knock down results in an expansion of the *slit2* expression domain in the commissural plate. Compiled confocal z-sections (A-C, G-I, M-O) or single 1μm optical slices (D-F, J-L) of wholemount zebrafish brains at 28hpf-30hpf. Rostral is facing and dorsal to the top in all panels. Embryos were injected with Std-cont MO (A-F), *zfzd3a*-UTR MO (G-L) or *zfzd3a*-AUG MO (M-O). *slit2* RNA expression (A, D, G, J, M; and in red in C, F, I, L, O) is shown in relation to formation of the axon scaffold labeled with HNK-1 (B, E, H, K, N; and in green in C, F, I, L, O). In control embryos *slit2* expression is restricted to the midline in a region dorsal to the optic recess (A-C). Single optical slices reveal that anterior commissural axons (arrowhead in E) cross the midline in a region devoid of *slit2* expression (as delineated by the bracket in panel D; also see merged image in F). Injection of *zfzd3a*-UTR MO or *zfzd3a*-AUG MO resulted in expansion of the *slit2* expression domain in the commissural plate (compare outline in G and M with that in A). Expansion of *slit2* at the region of commissure formation correlated with a failure of the AC to cross the midline (H, N, unfilled arrows; see also I and O). Single optical slices show *slit2* expression now extending into the region where the anterior

commissure (unfilled arrows K; also see merged image in L) would normally cross the rostral midline (compare J and K to D and E, respectively). Scale bar in C is 20μm.

Fig. 5. Knock down of zFzd3a results in the malformation of the telencephalic-diencephalic boundary at the optic recess. Compiled confocal z-sections (A-C, G-I) or single 2μm optical slices (D-F, J-L) of wholemount zebrafish brains at 28-30hpf. Yellow boxed areas in B and H are shown as single confocal slices in D-F and J-L respectively. Rostral is facing and dorsal to the top in all panels. Embryos were injected with Std-cont MO (A-F) or *zfzd3a*-AUG MO (G-L). Embryos were stained for *shh* RNA expression (A, D, G, J, and in red in C, F, I, L, O) and anti-acetylated tubulin (B, E, H, K; and in red C, F, I, L). In control embryos *shh* is normally expressed in the diencephalon, in a triangular domain underlying the POC with its apex just below the optic recess (A, D; and in red C, F). A small group of cells in the telencephalon are also positive for shh expression (dashed yellow outline, A). Embryos injected with zfzd3a-AUG MO that show commissural defects (unfilled arrowhead in H) show normal expression of *shh* in both the diencephalon (G, J; and in red I, L) and in the telencephalon (dashed yellow outline in G). In addition to staining the commissural axon, anti-acetylated α−tubulin also demarcates cell membranes. In control embryos a clear demarcation between the basal surface of telencephalic cells and the apical surface of diencephalic neuroepithelial cells is evident (filled arrowhead in E). However following knock down of zFzd3a a cluster of cells that have failed to integrate into the surrounding neuroepithelium are present at the junction of the telencephalon and diencephalon (filled arrowheads in K). Scale bar in C and F are 20μm.

Fig. 6. Abnormal patterning of *netrin* 1a expression domain following knock down of zFzd3a. Confocal z-series of wholemount zebrafish brains at 28-30hpf. Rostral is facing and dorsal is to the top in all images. Embryos were injected with Std-cont MO (A) or *zfzd3a*-AUG MO. Expression of *netrin1a* (A, G and in red C, I) is evident in a strip of cells above the optic recess and more caudally in cells adjacent to the rostral midline. Following knock down of zFzd3a, *netrin1a* expression expands into areas normally absent for *netrin1a* (compare filled arrows A and G). Scale bar in F is 20μm.

Fig. 7. Knock down of Slit2 rescues the anterior commissure phenotype. Confocal z-series of wholemount zebrafish brains at 28hpf stained with anti-acetylated tubulin to visualise axons. Rostral is facing and dorsal is to the top in all images. Embryos were injected with Std-cont MO (A), *slit2*-AUG MO (B, C), *zfzd3a*-AUG MO (D,E) or a combination of *zfzd3a*-AUG MO and *slit2*-AUG MO (F, G). The anterior commissure developed normally in embryos injected with Std-cont MO. Injection with *slit2*-AUG MO caused axons to project inappropriately in the neuroepithelium between the two commissures (unfilled arrowheads in B, C). In addition to this phenotype, some *slit2*-AUG MO injected embryos also showed a marked reduction of the anterior commissure (unfilled arrow in C). Knock down of zFzd3a resulted in a complete (arrow in D) or partial loss (arrow in E) of the anterior commissure. Knocking down both Slit2 and zFzd3a resulted in a significant decrease in embryos with a complete loss of the anterior commissure (arrow in F). Instead many axons now crossed the anterior commissure in these embryos (G). Knock down of Slit2 and zFzd3a did not affect the extent of axon wandering in between the commissures (unfilled arrowheads in F and G). Scale bar in A is 20μm.

Fig. 8. Working model for the role of zFzd3a in midline axon crossing in the commissural plate. (A) In wild type embryos axons in the anterior commissure grow across the midline surrounded by glia (green). The chemorepulsive Slit2 expressing cells (red) lie deep to the tract. (B) Following knock down of zFzd3a, the region of Slit2 expression is expanded due to malformation of the commissural plate. This expansion of Slit2 disrupts the axon growth substrate, in particular glia. In addition to perturbation of the growth substrate Slit2 also acts as a repulsive cue for axons. Thus axons stall and fail to cross the midline.

References

Abramoff MD, Magelhaes PJ, Ram SJ (2004) Image processing with ImageJ. Biophotonics International 11:36-42.

Akimenko MA, Ekker M, Wegner J, Lin W, Westerfield M (1994) Combinatorial expression of three zebrafish genes related to distal-less: part of a homeobox gene code for the head. J Neurosci 14:3475-3486.

Barresi MJ, Hutson LD, Chien CB, Karlstrom RO (2005) Hedgehog regulated Slit expression determines commissure and glial cell position in the zebrafish forebrain. Development 132:3643-3656.

Bhanot P, Brink M, Samos CH, Hsieh JC, Wang Y, Macke JP, Andrew D, Nathans J, Nusse R (1996) A new member of the frizzled family from Drosophila functions as a Wingless receptor. Nature 382:225-230.

Briancon-Marjollet A, Ghogha A, Nawabi H, Triki I, Auziol C, Fromont S, Piche C, Enslen H, Chebli K, Cloutier JF, Castellani V, Debant A, Lamarche-Vane N (2008) Trio mediates netrin-1-induced Rac1 activation in axon outgrowth and guidance. Mol Cell Biol 28:2314-2323.

Chitnis AB, Kuwada JY (1990) Axonogenesis in the brain of zebrafish embryos. J Neurosci 10:1892-1905.

Ciruna, B., Jenny, A., Lee, D., Mlodzik, M., and Schier, A.F. (2006) Planar cell polarity signalling couples cell division and morphogenesis during neurulation. Nature 439(7073):220-224

Danesin C, Peres JN, Johansson M, Snowden V, Cording A, Papalopulu N, Houart C (2009) Integration of telencephalic Wnt and hedgehog signaling center activities by Foxg1. Dev Cell 16:576-587.

Dann CE, Hsieh JC, Rattner A, Sharma D, Nathans J, Leahy DJ (2001) Insights into Wnt binding and signalling from the structures of two Frizzled cysteine-rich domains. Nature 412:86-90.

Devine CA, Key B (2003) Identifying axon guidance defects in the embryonic zebrafish brain. Methods Cell Sci 25:33-37.

Falk J, Bechara A, Fiore R, Nawabi H, Zhou H, Hoyo-Becerra C, Bozon M, Rougon G, Grumet M, Puschel AW, Sanes JR, Castellani V (2005) Dual functional activity of semaphorin 3B is required for positioning the anterior commissure. Neuron 48:63-75.

Fazeli A, Dickinson SL, Hermiston ML, Tighe RV, Steen RG, Small CG, Stoeckli ET, Keino-Masu K, Masu M, Rayburn H, Simons J, Bronson RT, Gordon JI, Tessier-Lavigne M, Weinberg RA (1997) Phenotype of mice lacking functional Deleted in colorectal cancer (Dcc) gene. Nature 386:796-804.

Fjose A, Izpisua-Belmonte JC, Fromental-Ramain C, Duboule D (1994) Expression of the zebrafish gene hlx-1 in the prechordal plate and during CNS development. Development 120:71-81.

Frohman MA, Dush MK, Martin GR (1988) Rapid production of full-length cDNAs from rare transcripts: amplification using a single gene-specific oligonucleotide primer. Proc Natl Acad Sci U S A 85:8998-9002.

Gerety SS, Wilkinson DG (2011) Morpholino artifacts provide pitfalls and reveal a novel role for pro-apoptotic genes in hindbrain boundary development. Dev biol 350: 279-289d

Hjorth JT, Key B (2001) Are pioneer axons guided by regulatory gene expression domains in the zebrafish forebrain? High-resolution analysis of the patterning of the zebrafish brain during axon tract formation. Dev Biol 229:271-286.

Hjorth J, Key B (2002) Development of axon pathways in the zebrafish central nervous system. Int J Dev Biol 46:609-619.
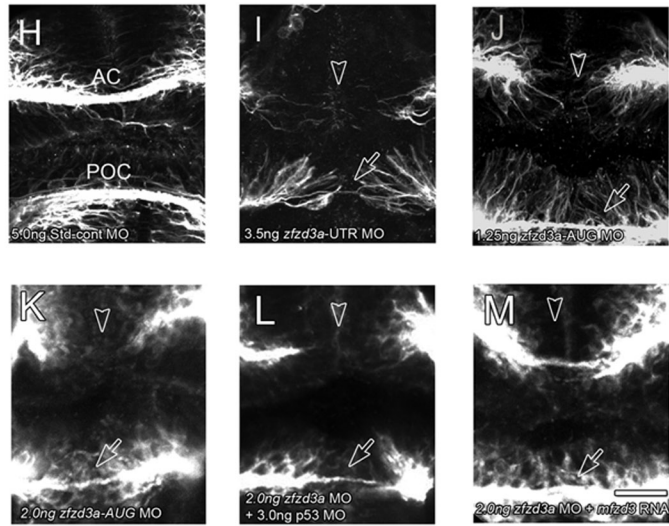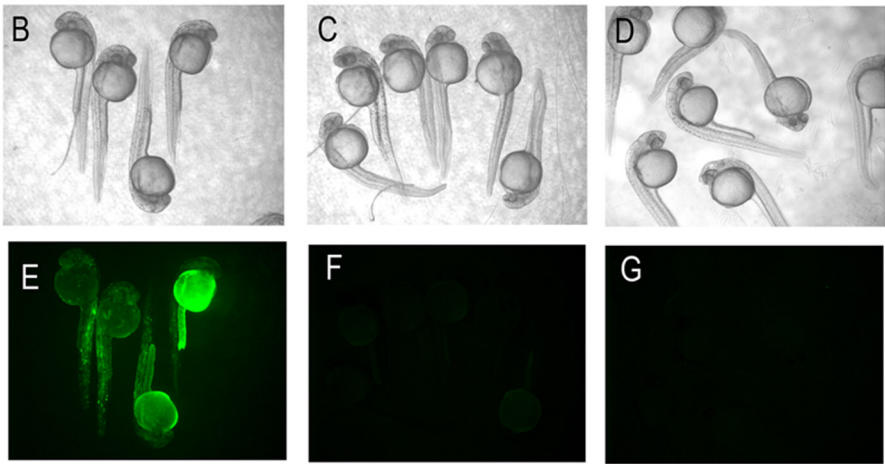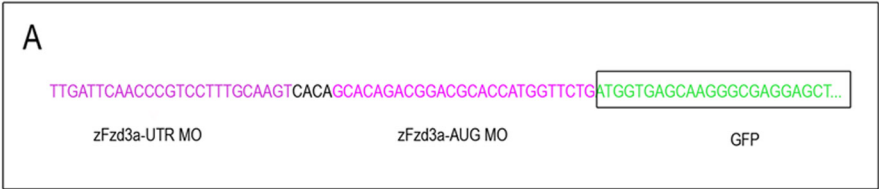
Houart C, Caneparo L, Heisenberg C, Barth K, Take-Uchi M, Wilson S (2002) Establishment of the telencephalon during gastrulation by local antagonism of Wnt signaling. Neuron 35:255-265.

Hutson LD, Chien CB (2002) Pathfinding and error correction by retinal axons: the role of astray/robo2. Neuron 33:205-217.

Hutson LD, Jurynec MJ, Yeo SY, Okamato H, Chien CB (2003) Two divergent slit genes in zebrafish. Dev Dyn 228(3): 358-369.

Ille F, Sommer L (2005) Wnt signaling: multiple functions in neural development. Cell Mol Life Sci 62:1100-1108.

Kassai H, Terashima T, Fukaya M, Nakao K, Sakahara M, Watanabe M, Aiba A (2008) Rac1 in cortical projection neurons is selectively required for midline crossing of commissural axonal formation. Eur J Neurosci 28:257-267.

Kawahara A, Dawid IB (2002) Developmental expression of zebrafish emx1 during early embryogenesis. Gene Expr Patterns 2:201-206.

Kim SH, Shin J, Park Hc, Yeo SY, Hong SK, Han S, Rhee M, Kim CH, Chitnis AB, Huh TL (2002) Specification of an anterior neuroectoderm patterning by Frizzled8a-mediated Wnt8b signalling during late gastrulation in zebrafish. Development 129(19) 4443-4455.

Krauss S, Concordet JP, Ingham PW (1993) A functionally conserved homolog of the Drosophila segment polarity gene hh is expressed in tissues with polarizing activity in zebrafish embryos. Cell 75:1431-1444.

Krauss S, Johansen T, Korzh V, Fjose A (1991) Expression pattern of zebrafish pax genes suggests a role in early brain regionalization. Nature 353:267-270.
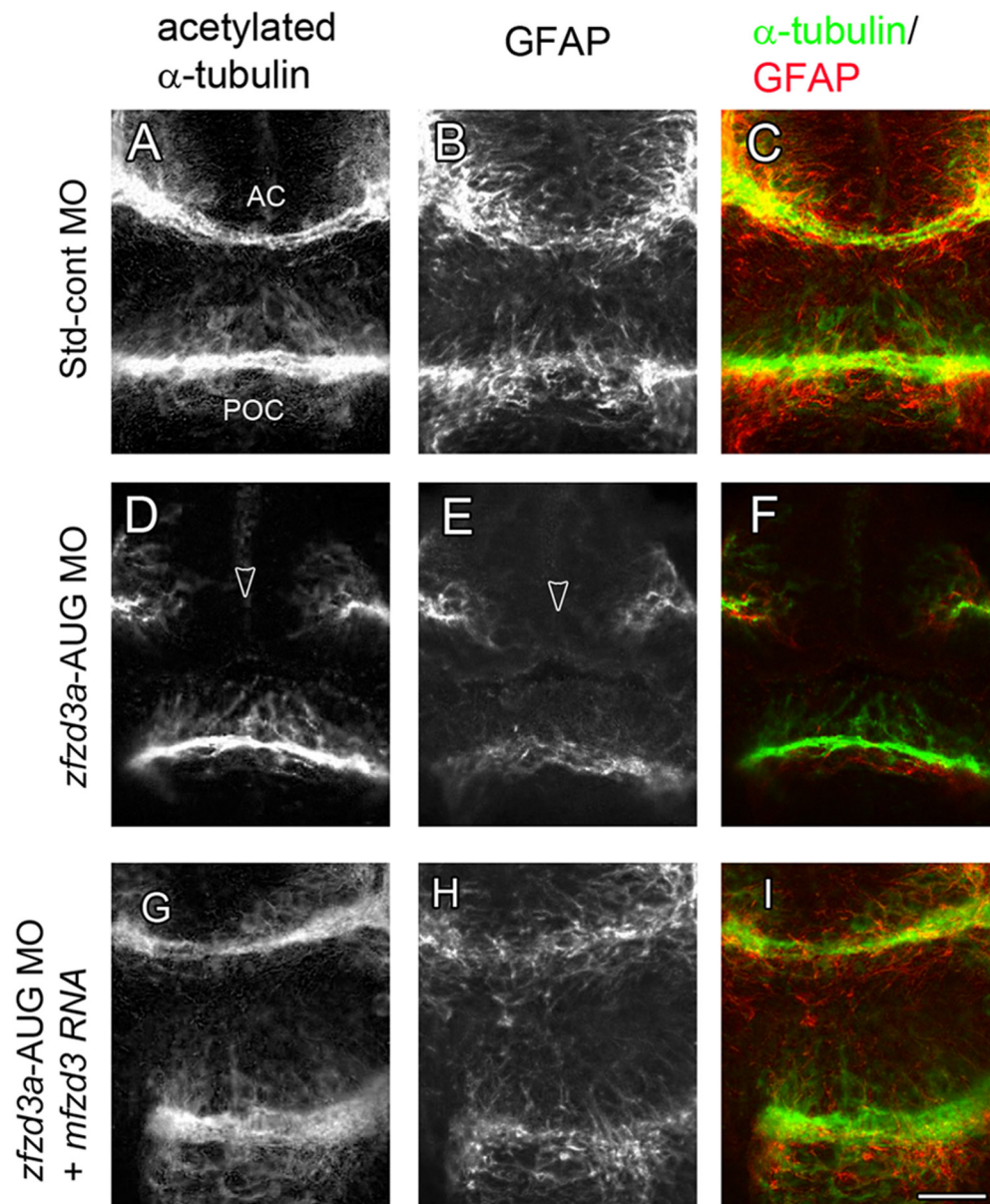
Kullander K, Mather NK, Diella F, Dottori M, Boyd AW, Klein R (2001) Kinase-dependent and kinase-independent functions of EphA4 receptors in major axon tract formation in vivo. Neuron 29:73-84.

Lauderdale, J.D., Davis, N.M., and Kuwada, J.Y. (1997) Axon tracts correlate with Netrin-1a expression in the zebrafish embryo. Mol. Cell Neurosci. 9(4):293-313

Lindwall C, Fothergill T, Richards LJ (2007) Commissure formation in the mammalian forebrain. Curr Opin Neurobiol 17:3-14.

Lyuksyutova AI, Lu CC, Milanesio N, King LA, Guo N, Wang Y, Nathans J, Tessier-Lavigne M, Zou Y (2003) Anterior-posterior guidance of commissural axons by Wnt-frizzled signaling. Science 302:1984-1988.

Miyasaka N, Sato Y, Yeo SY, Hutson LD, Chien CB, Okamato H, Yoshihara Y (2005) Robo2 is required for the establishment of a precise glomerular map in the zebrafish olfactory system. Development 132 (6): 1283-1293.

Molven A, Njolstad PR, Fjose A (1991) Genomic structure and restricted neural expression of the zebrafish wnt-1 (int-1) gene. Embo J 10:799-807.

Nona SN, Shehab SAS, Stafford CA, Cronly-Dillon JR (1989) Glial fibrillary acidic protein (GFAP) from goldfish: Its localisation in visual pathway. Glia 2:189-200

Robu ME, Larson JD, Nasevicus A, Beiraghi S, Brenner C, Farber SA, Ekker SC (2007) p53 activation by knock down technologies. PLoS Genet 3:e78

Ross LS, Parrett T, Easter SS, Jr. (1992) Axonogenesis and morphogenesis in the embryonic zebrafish brain. J Neurosci 12:467-482.

Serafini T, Colamarino SA, Leonardo ED, Wang H, Beddington R, Skarnes WC, Tessier-Lavigne M (1996) Netrin-1 is required for commissural axon guidance in the developing vertebrate nervous system. Cell 87:1001-1014.

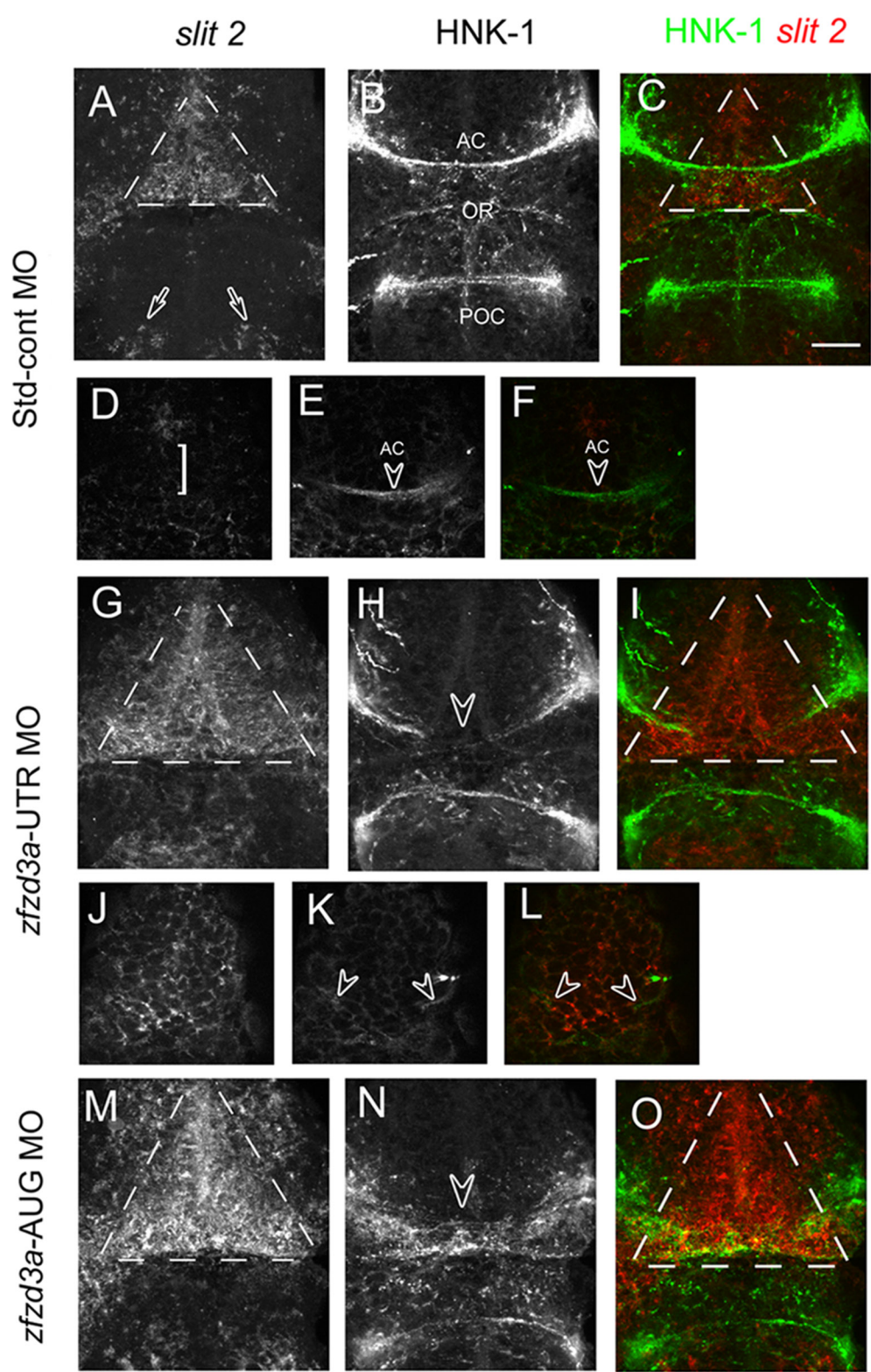Strähle, U., Fischer, N., and Blader, P. (1997) Expression and regulation of a netrin homologue in the zebrafish embryo. Mech. Dev. 62(2):147-160

Suto F, Ito K, Uemura M, Shimizu M, Shinkawa Y, Sanbo M, Shinoda T, Tsuboi M, Takashima S, Yagi T, Fujisawa H (2005) Plexin-a4 mediates axon-repulsive activities of both secreted and transmembrane semaphorins and plays roles in nerve fiber guidance. J Neurosci 25:3628-3637.

Turner DL, Weintraub H (1994) Expression of achaete-scute homolog 3 in Xenopus embryos converts ectodermal cells to a neural fate. Genes Dev 8:1434-1447.

Wada H, Tanaka H, Nakayama S, Iwasaki M, Okamato H (2006) Frizzled3a and Celsr2 function in the neuroepithelium to regulate migration of facial motor neurons in the developing zebrafish hindbrain. Development 133(23): 4749-4759.

Wang Y, Guo N, Nathans J (2006a) The role of Frizzled3 and Frizzled6 in neural tube closure and in the planar polarity of inner-ear sensory hair cells. J Neurosci 26:2147-2156.

Wang Y, Zhang J, Mori S, Nathans J (2006b) Axonal growth and guidance defects in Frizzled3 knock-out mice: a comparison of diffusion tensor magnetic resonance imaging, neurofilament staining, and genetically directed cell labeling. J Neurosci 26:355-364.

Wang Y, Thekdi N, Smallwood PM, Macke JP, Nathans J (2002) Frizzled-3 is required for the development of major fiber tracts in the rostral CNS. J Neurosci 22:8563-8573.

Widelitz R (2005) Wnt signaling through canonical and non-canonical pathways: recent progress. Growth Factors 23:111-116.

Wilson SW, Easter SS, Jr. (1991) A pioneering growth cone in the embryonic zebrafish brain. Proc Natl Acad Sci U S A 88:2293-2296.

Xiao, T., Staub, W., Robles, E., Gosse, N.J., Cole, G.J., and Baier, H. (2011) Assembly of Lamina-Specific Neuronal Connections by Slit Bound to Type IV Collagen. Cell 146(1):164-176
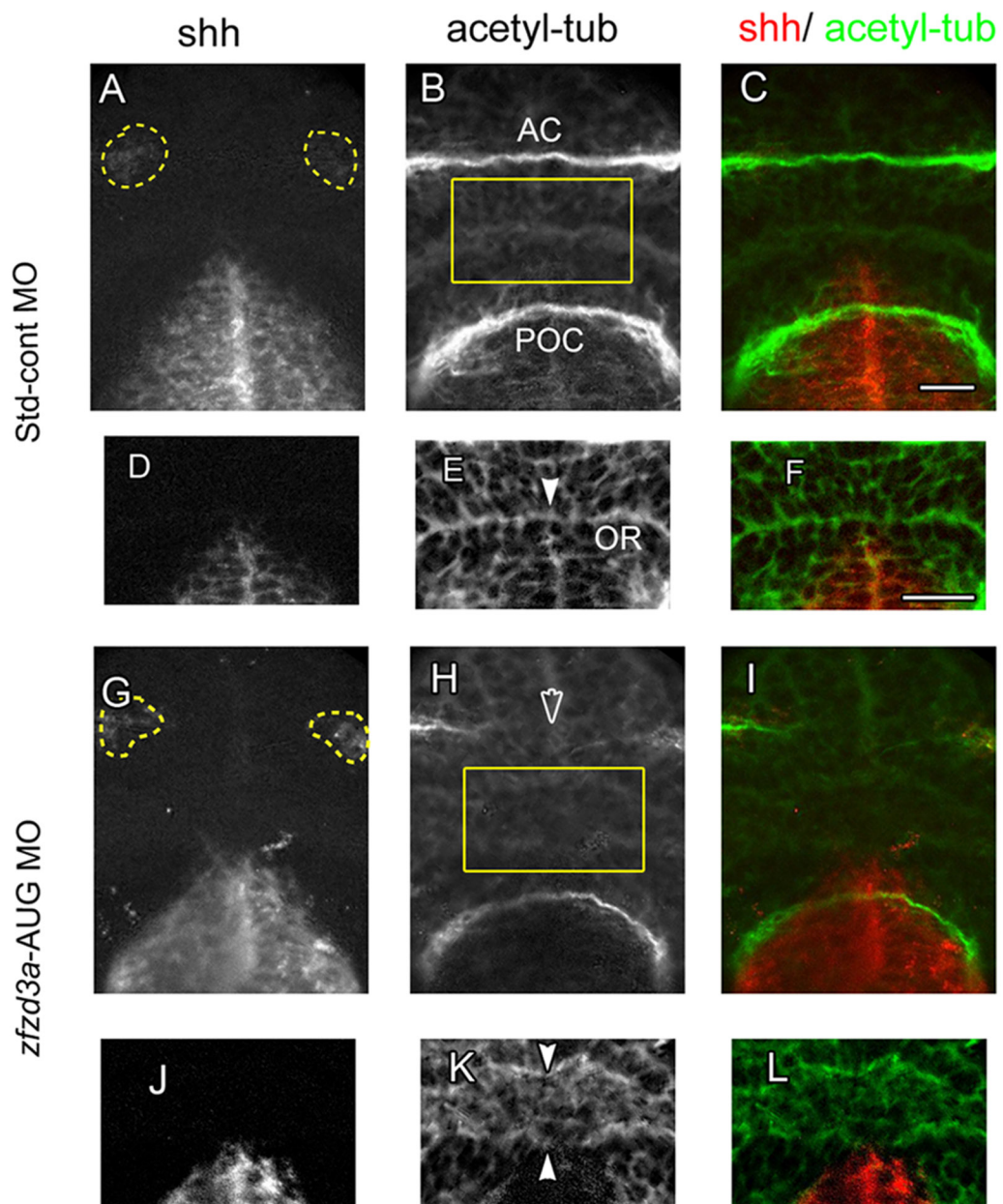
Zhou L, Bar I, Achouri Y, Campbell K, De Backer O, Hebert JM, Jones K, Kessaris N, de Rouvroit CL, O'Leary D, Richardson WD, Goffinet AM, Tissir F (2008) Early forebrain wiring: genetic dissection using conditional Celsr3 mutant mice. Science 320:946-949.
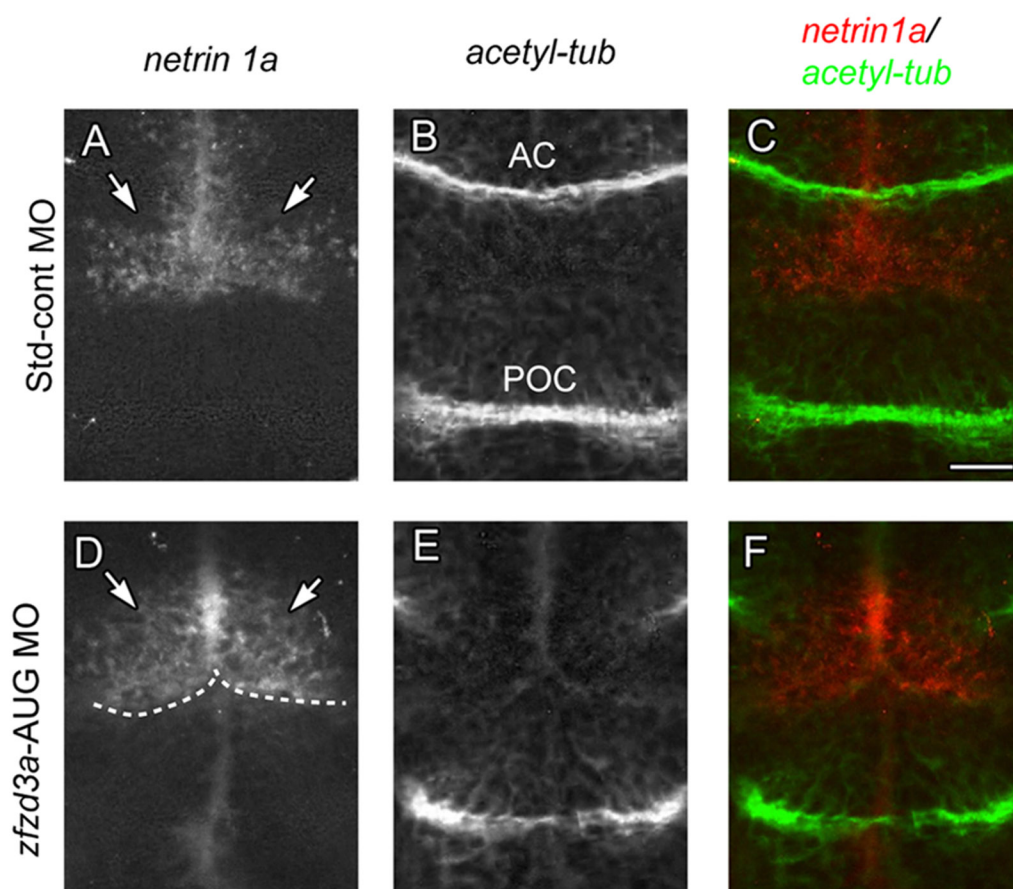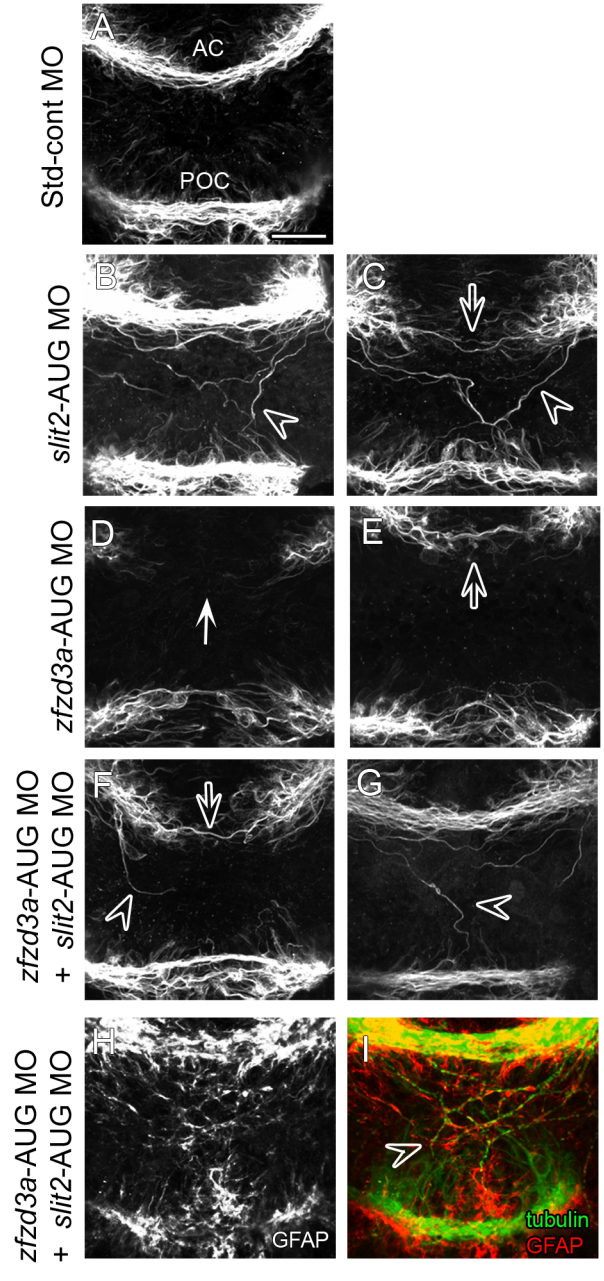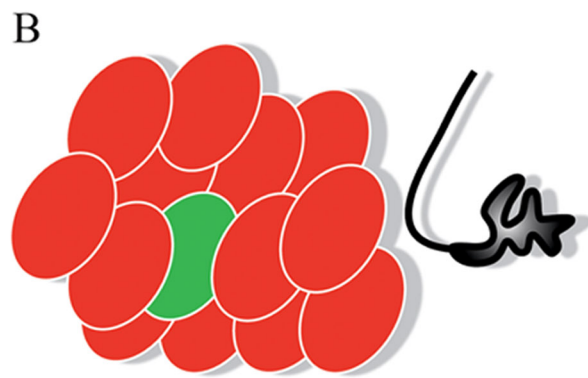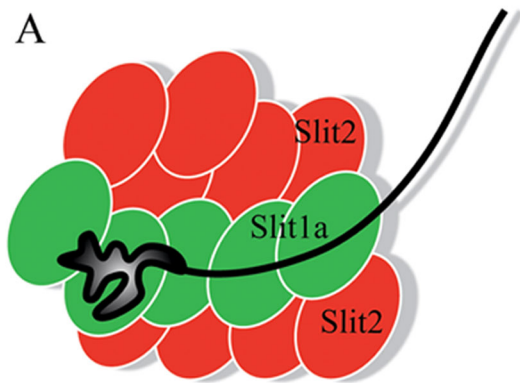
A

ec
drc
PC
AC
SOT
DVDT
TPC
OR
TPOC
vrc
vcc
MLF
POC
VC

B

te
mes
di
rh
OR

zfzd3a Riboprobe

C

AC
OR
HNK-1 POC

D

zfzd3a Riboprobe

E

Merge

F

HNK-1

G

sense control

H

Merge

A

TTGATTCAACCCGTCCTTTGCAAGTCACAGCACAGACGGACGCACCATGGTTCTGATGGTGAGCAAGGGCGAGGAGCT...

zFzd3a-UTR MO   zFzd3a-AUG MO   GFP

acetylated
α-tubulin

GFAP

α-tubulin/
GFAP

Std-cont MO

AC

POC

A

B

C

zfzd3a-AUG MO

D

E

F

zfzd3a-AUG MO
+ mfzd3 RNA

G

H

I

| | *slit 2* | HNK-1 | HNK-1 *slit 2* |

	shh	acetyl-tub	shh/ acetyl-tub
Std-cont MO	A	B AC / POC	C
	D	E OR	F
zfzd3a-AUG MO	G	H	I
	J	K	L

	netrin 1a	*acetyl-tub*	*netrin1a*/ *acetyl-tub*
Std-cont MO	A	B AC / POC	C
zfzd3a-AUG MO	D	E	F

Std-cont MO

AC

POC

slit2-AUG MO

zfzd3a-AUG MO

zfzd3a-AUG MO + *slit2*-AUG MO

zfzd3a-AUG MO + *slit2*-AUG MO

GFAP

tubulin
GFAP

A

Slit2
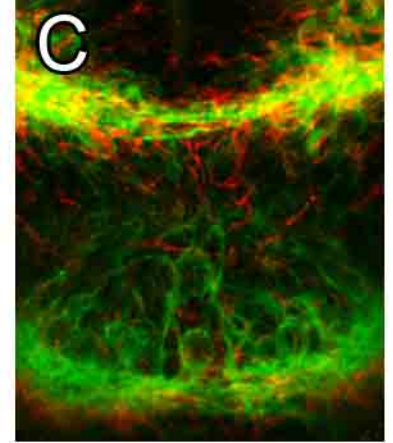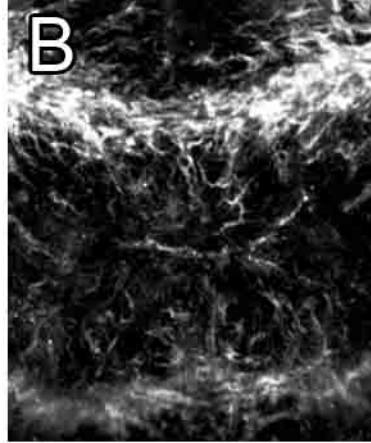
Slit1a

Slit2

B

slit 1a   HNK-1   *HNK-1* *slit 1a*

Std cont MO

zfzd3a-AUG MO +
p53 MO

| | *netrin 1b* | *acetyl-tub* | *netrin 1b*/
acetyl-tub |

A Std-cont MO hlx B zfzd3a MO hlx C Std-cont MO wnt1 D zfzd3a MO wnt1

E Std-cont MO shh F zfzd3a MO shh G Std-cont MO shh H zfzd3a MO shh

I Std-cont MO dlx2 J zfzd3a MO dlx2 K Std-cont MO pax6 L zfzd3a MO pax6
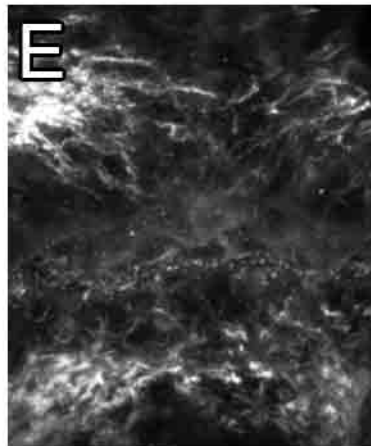
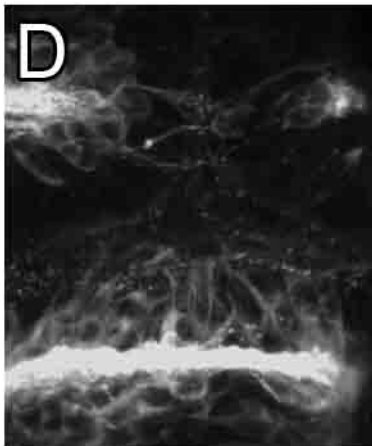M Std-cont MO emx N zfzd3a MO emx
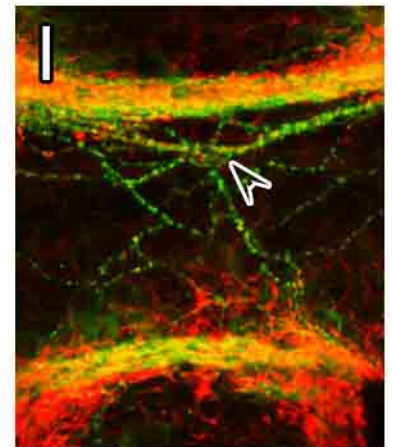
acetylated α-tubulin
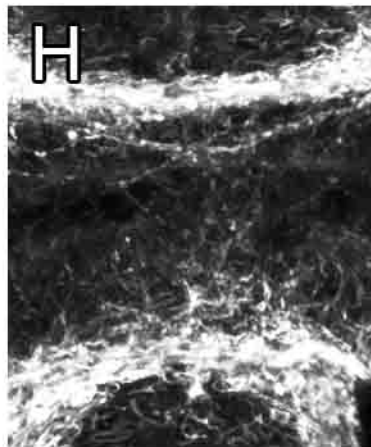
GFAP

α-tubulin/ GFAP

Std-cont MO

zfzd3a-AUG MO
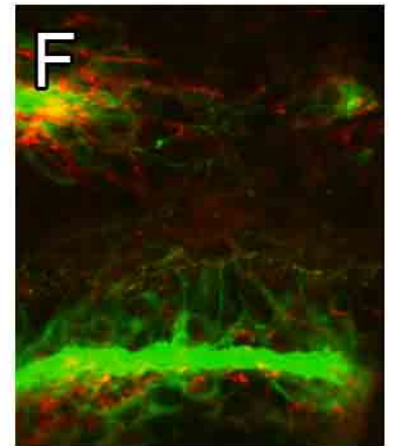
slit2-AUG MO

Supplementary Fig. 1.. Knock down of zFzd3a reduced expression of *slit1a* at the midline.

Embryos were injected with Std-cont MO (A-F), zFzd3a-UTR MO or zFzd3a-AUG MO (G-I) and co-stained for expression of *slit1a* (A, D and G) and HNK-1 (B, E and H). C, F and I are merged images of A-B, D-E and G-H, respectively. HNK-1 staining is green and *slit1a* expression is red. Rostral is facing and dorsal to the top in all panels. (A-C) In wild-type embryos *slit1a* appears to be expressed in cells surrounding both the anterior commissure (AC) and the post-optic commissure (POC). (D-F) Single 1μm optical slices at the same level from the complied z-sections in panels A-C. Anterior commissure axons cross the midline by passing between *slit1a* expressing neuroepithelial cells. *slit1a* expression is reduced and the anterior commissure is absent following knock down of zFzd3a with either the zfzd3a-UTR or the zfzd3a-AUG MO (G-I). At the midline the expression of *slit1a* is almost completely absent (unfilled arrow,G), being confined to regions adjacent to the midline (dashed outline, G). The defasciculation of the post-optic commissure (filled arrowhead, H) correlates with reduced expression of *slit1a* in cells surrounding this tract. Scale bar in C is 20μm.

Supplementary Fig. 2. High resolution confocal microscopy reveals the presence of aberrant cells at the telencephalic/diencephalic boundary. Single 2μm optical slices (A-B) of wholemount zebrafish brains at 28-30hpf. Rostral is facing and dorsal to the top in all panels. Embryos were injected with Std-cont MO (A) or zFzd3a-AUG MO and p53 MO). In control embryos background staining from anti-α-acetylated tubulin shows a clear boundary between the

telencephalon and diencephalon (filled arrowhead in A). Following injection with zFzd3a-AUG MO and p53 MO to control for any potential off-target effects a cluster of cells are present between the telencephalon and diencephalon (filled arrowheads in B). Similar to injection of zFzd3a-AUG MO alone. Scale bar in C is 20μm.

Supplementary Fig. 3. Expression of *netrin1b* in the rostral midline. *Netrin1b* (D,J and in red F,L) is present at the rostral midline in a domain similar to *slit2* it is also expressed in more lateral areas of the forebrain (data not shown). Following knock down of zFzd3a, *netrin 1b* is still expressed at the rostral midline but in a broader domain as the the midline itself fails to form properly (unfilled arrow D, J) due to the presence of disorganized cells at the telencephalic/diencephalic boundary (unfilled arrowheads K) not evident in control embryos (unfilled arrowhead E). Scale bar in C is 20μm.

Supplementary Fig. 4. Gene expression patterns of region specific markers in the brains of control and *zfzd3a* morpholino injected embryos. Embryos were injected with Std-cont MO (A, C, E, G, I, K, M) or zfzd3a MO (B, D, F, H, J, L, N) and stained for expression of forebrain region specific markers. In the caudal diencephalon and in the mesencephalon the expression of *hlx* remained unchanged following knock down of zFzd3a (A, B). Formation of the MHB boundary also appeared normal in zFzd3a MO injected embryos as indicated by expression of *wnt1* (C-D). *Shh* shows normal expression in the hypothalamus of Fzd3a-MO injected embryos but is reduced in the zona limitans intrathalamica in 29% of embryos (E-H). Expression of *dlx2* and *pax6.1* in the telencephalon and in the ventral thalamus remained unaltered in zFzd3a MO injected embryos (I-L). Similarly no change was seen in the expression of *emx* in the more dorsal

region of the telencephalon (K, L). Lateral views with rostral to the left are shown for all panels except for G and H which are anterior views.

Supplementary Fig 5. GFAP staining following separate knockdown of zFzd3a or Slit2. Embryos injected with std-cont MO show normal expression of acetylated tubulin (A) and GFAP (B). In embryos injected with *zfzd3a*-AUG MO an absence of axons crossing at the AC is accompanied by an absence of glial cells at the AC (D-E). Injection of slit2 (G-I) shows association of glial cells with axons that have wandered between commissures (arrowhead, I), but an otherwise normal formation of the glial bridge and AC.